

Caveolin Transfection Results in Caveolae Formation but Not Apical Sorting of Glycosylphosphatidylinositol (GPI)-anchored Proteins in Epithelial Cells

Concetta Lipardi,* Rosalia Mora,[‡] Veronica Colomer,[‡] Simona Paladino,* Lucio Nitsch,* Enrique Rodriguez-Boulan,[‡] and Chiara Zurzolo*

*Centro di Endocrinologia ed Oncologia Sperimentale del Consiglio Nazionale delle Ricerche, Dipartimento di Biologia e Patologia Cellulare e Molecolare, Università degli Studi di Napoli Federico II, 80131 Napoli, Italy; and[‡]Margaret Dyson Vision Research Institute and Department of Cell Biology, Cornell University Medical College, New York 10021

Abstract. Most epithelial cells sort glycosylphosphatidylinositol (GPI)-anchored proteins to the apical surface. The “raft” hypothesis, based on data mainly obtained in the prototype cell line MDCK, postulates that apical sorting depends on the incorporation of apical proteins into cholesterol/glycosphingolipid (GSL) rafts, rich in the cholesterol binding protein caveolin/VIP21, in the Golgi apparatus. Fischer rat thyroid (FRT) cells constitute an ideal model to test this hypothesis, since they missort both endogenous and transfected GPI-anchored proteins to the basolateral plasma membrane and fail to incorporate them into cholesterol/glycosphingolipid clusters. Because FRT cells lack caveolin, a major component of the caveolar coat that has been proposed to have a role in apical sorting of GPI-anchored proteins (Zurzolo, C., W. Van’t Hoff, G. van Meer, and E. Rodriguez-Boulan. 1994. *EMBO [Eur.*

Mol. Biol. Organ.] J. 13:42–53.), we carried out experiments to determine whether the lack of caveolin accounted for the sorting/clustering defect of GPI-anchored proteins. We report here that FRT cells lack morphological caveolae, but, upon stable transfection of the *caveolin1* gene (*cav1*), form typical flask-shaped caveolae. However, *cav1* expression did not redistribute GPI-anchored proteins to the apical surface, nor promote their inclusion into cholesterol/GSL rafts. Our results demonstrate that the absence of caveolin1 and morphologically identifiable caveolae cannot explain the inability of FRT cells to sort GPI-anchored proteins to the apical domain. Thus, FRT cells may lack additional factors required for apical sorting or for the clustering with GSLs of GPI-anchored proteins, or express factors that inhibit these events. Alternatively, *cav1* and caveolae may not be directly involved in these processes.

EPITHELIAL cells are characterized by the presence of polarized plasma membrane domains with different compositions of proteins and lipids (Rodriguez-Boulan and Powell, 1992; Eaton and Simons, 1995; Drubin and Nelson, 1996). In recent years, several sorting signals have been identified that mediate localization of proteins to apical or basolateral plasma membrane domains (Mostov et al., 1992; Matter and Mellman, 1994; Le Gall et al., 1995). Whereas basolateral signals are short, discrete sequences localized in the cytoplasmic domain of the protein, the best characterized apical signal is a glycosphingolipid, glycosylphosphatidylinositol (GPI)¹ (Lisanti

and Rodriguez-Boulan, 1990), which is used by some proteins as an anchor to the membrane bilayer (Cross, 1987; Ferguson and Williams, 1988; Low and Saltiel, 1988; Low, 1989; Doering et al., 1990; Lisanti et al., 1990). GPI-anchored proteins are selectively localized to the apical membrane of most epithelial cells studied to date (Lisanti et al., 1988; Ali and Evans, 1990; Lisanti et al., 1990; Wilson et al., 1990). Furthermore, a GPI anchor is sufficient to target recombinant GPI-anchored proteins to the apical membrane of MDCK cells (Brown et al., 1989; Lisanti et al., 1989).

Attachment of the GPI moiety occurs in the luminal face of the endoplasmic reticulum by enzymatic replacement of COOH-terminal sequences that act as signals for GPI anchoring (for review see Englund, 1993; McConville and Ferguson, 1993; Vidugiriene and Menon, 1995). The newly synthesized GPI-anchored proteins are then transported to the cell surface, where they are exposed on the topologically equivalent extracytoplasmic face of the plasma membrane (Vidugiriene and Menon, 1994). Sorting of GPI-anchored proteins occurs after their carbohydrates are processed in the Golgi complex (Brown et al., 1989;

Address all correspondence to Chiara Zurzolo, Dipartimento di Biologia e Patologia e Molecolare, II Facoltà di Medicina, Via Pansini 5, 80131 Napoli, Italy. Tel.: (81) 746-32-37. Fax: (81) 770-10-16. E-mail: zurzolo@ds.unina.it

1. *Abbreviations used in this paper:* *cav1*, *caveolin 1*; CMV, cytomegalovirus; DAF, decay accelerating factor; FRT, Fischer rat thyroid; GPI, glycosylphosphatidylinositol; GSL, glycosphingolipid; TIFF, Triton-insoluble floating fraction; TX-100, Triton X-100.

Lisanti et al., 1989), presumably by incorporation into post-Golgi vesicles assembled in the TGN (Lisanti and Rodriguez-Boulan, 1990; Wandinger-Ness et al., 1990).

As they migrate through the proximal Golgi complex, GPI-anchored proteins undergo a dramatic change in their biophysical properties, reflected by their becoming insoluble in certain nonionic detergents, such as Triton X-100 (TX-100) (Brown and Rose, 1992; Garcia et al., 1993; Zurzolo et al., 1994). This appears to reflect the association of GPI-anchored proteins with glycosphingolipid-cholesterol clusters in the Golgi complex, which are also detergent insoluble (Thompson and Tillack, 1985). When purified by flotation in sucrose density gradients, these aggregates, denoted TIFF (Triton-insoluble floating fraction; Kurzchalia et al., 1995) or detergent-insoluble glycosphingolipid-enriched domains (DIG; Parton, 1996) can be shown to be rich in GPI-anchored proteins, sphingomyelin, glycosphingolipids (GSL)s and cholesterol (Brown and Rose, 1992; Garcia et al., 1993; Sargiacomo et al., 1993; Zurzolo et al., 1994). Fluorescence energy transfer experiments indicate that GPI-anchored proteins are still clustered when they arrive at the cell surface, but slowly disperse in the next few hours (Hannan et al., 1993).

The "raft hypothesis" postulates that clustering with GSLs is required for the sorting of apical proteins (Simons and Ikonen, 1997; van Meer and Simons, 1988). GSLs are sorted apically in MDCK (kidney) and Caco-2 (intestinal) epithelial cells, at least as indicated by experiments with short acyl chain fluorescent glycolipids (van Meer et al., 1987; van't Hof and van Meer, 1990). In its extended version, the raft includes transmembrane apical proteins, such as influenza hemagglutinin, which also becomes detergent insoluble as it traverses the Golgi complex (Skibbens et al., 1989). The mechanisms involved in the formation of the raft are still obscure. The length and saturation of the acyl chains of GSLs appear to be important in this process (Schroeder et al., 1994). A similar GSL-cholesterol enrichment as in the Golgi raft was reported for plasma membrane caveolae (Fra et al., 1994; Gorodinski et al., 1995; Kurzchalia et al., 1995; Mayor et al., 1995; Parton, 1996; Schnitzer et al., 1995b). Initial reports suggested that GPI-anchored proteins are also enriched in caveolae (Rothberg et al., 1990; Sargiacomo et al., 1993); however, recent evidence suggests that GPI-anchored proteins are distributed evenly throughout the plasma membrane, but redistribute to caveolar regions upon cross-linking, e.g., with antibodies (Mayor et al., 1994; Parton et al., 1994; Schnitzer et al., 1995a). Caveolae are coated on the cytoplasmic side by a coat that includes a phosphorylated cholesterol-binding protein of 21 kD, caveolin (Rothbergh et al., 1992; Murata et al., 1995). Recent transient transfection experiments in lymphocytes indicate that caveolin is required for the assembly of morphological caveolae (Fra et al., 1995). The observations that caveolin is identical to VIP21, a protein present in post-Golgi vesicles and the TGN (Wandinger-Ness et al., 1990; Kurzchalia et al., 1992), and that caveolin localizes into TIFF (Sargiacomo et al., 1993; Zurzolo et al., 1994; Kurzchalia et al., 1995), suggest a possible involvement of this protein in the formation of post-Golgi transport vesicles (Dupree et al., 1993). However, caveolae have not been identified in the TGN to date.

The polarized epithelial cell line Fischer rat thyroid

(FRT) provides an excellent model to study the role of caveolin in both GPI-anchored protein sorting and caveolar assembly (Zurzolo et al., 1992; Nitsch et al., 1985). FRT cells do not express caveolin (Sargiacomo et al., 1993; Zurzolo et al., 1994) and do not form caveolae (this paper). Although FRT cells can sort transmembrane apical proteins to their correct plasma membrane domain (Zurzolo et al., 1992), they deliver endogenous and transfected GPI-anchored proteins and fluorescent GSLs to the basolateral membrane and fail to incorporate GPI proteins into TIFF (Zurzolo et al., 1993, 1994). In this paper, we report the results of experiments in which we transfected *caveolin1* (*cav1*) into FRT cells to examine its effect on GPI-anchored protein sorting, clustering, and caveolar assembly. Although caveolin was sufficient to promote the assembly of morphologically normal caveolae in FRT cells, it failed to redistribute GPI proteins to the apical surface or to affect their clustering into TIFF.

Materials and Methods

Reagents and Antibodies

Cell culture reagents were purchased from Gibco Laboratories (Grand Island, NY). Protein A-Sepharose was from Pharmacia Diagnostics AB (Uppsala, Sweden), sulfo-NHS derivatives and streptavidin-agarose beads were from Pierce Chemical Co. (Rockford, IL). The monoclonal antibody (MCA404) against herpes simplex virus was from Serotec Ltd. (Kidlington, Oxford, United Kingdom), anticaveolin polyclonal antibody was from Transduction Laboratories (Lexington, KY). Affinity-purified antibodies (rabbit anti-mouse IgG) were purchased from Cappel Laboratories (Malvern, PA). All other reagents were obtained from Sigma Chemical Co. (St. Louis, MO).

Cell Culture and Transfection

FRT cells stably expressing gD1-DAF (Zurzolo et al., 1993), and FRT cells expressing transfected *cav1* were grown in F12 Coon's modified medium containing 5% FBS. MDCK cells were maintained in DME supplemented with 5% FBS. FRT cells were cotransfected as previously described using a modification of the calcium phosphate precipitation procedure (Zurzolo et al., 1993). The VIP21/*cav1* cDNA from MDCK cells was a gift from P. Dupree (European Molecular Biology Laboratory, Heidelberg, Germany, [EMBL]) and was inserted into pCMV5, carrying the gene for resistance to G418, using the EcoRI and KpnI restriction sites. For some experiments we used myc-caveolin cDNA (from R.G.W. Anderson, University of Texas Health Science Center, Dallas, TX). The construct containing gD1-DAF under the Rous sarcoma virus promoter was a gift of I. Caras (Genentech Inc., South San Francisco, CA) and has been described elsewhere (Lisanti et al., 1989; Zurzolo et al., 1993).

Biotinylation Assays

Confluent monolayers on transwells were labeled overnight using 1 mCi/ml of [³⁵S]met-cys (Amersham Corp., Arlington Heights, IL), and were biotinylated and processed for immunoprecipitation as previously described (Le Bivic et al., 1989; Sargiacomo et al., 1989; Zurzolo et al., 1993). To recover the immunoprecipitated biotinylated antigens, the beads were boiled in 10 ml of 10% SDS for 5 min, diluted with lysis buffer, and then centrifuged for 1 min at 14,000 rpm. Biotinylated antigens present in the supernatants were precipitated with streptavidin-agarose beads. Finally, the beads were boiled in Laemmli buffer (Laemmli, 1970) and analyzed by SDS-PAGE. Dried gels were processed as described (Zurzolo et al., 1992) using preflashed films; densitometry analysis was carried out within the linear range of the film. The steady-state distribution of endogenous GPI-anchored proteins was determined using domain-selective biotinylation and treatment with phospholipase C, as previously described (Lisanti et al., 1988; Zurzolo et al., 1993).

Pulse-chase and TX-100 Extraction

TX-100 extractability during pulse-chase experiments was assayed as pre-

viously described (Brown and Rose, 1992; Zurzolo et al., 1994). Briefly, cells that had just reached confluency in 35-mm dishes were starved of methionine and cysteine for 20 min, pulse labeled for 5 min with 100 ml of pulse medium containing ~500 mCi/ml of [³⁵S]met-cys, and then incubated in chase medium (DME containing 10% FBS and 100X met and cys) for different times. After each time point, cells were washed twice with PBS containing 1 mM CaCl₂ and 1 mM MgCl₂ (PBS CM) on ice as described previously, and then lysed for 20 min on ice in 1 ml TNE/TX-100 buffer (Brown and Rose, 1992; Zurzolo et al., 1994). Lysates were collected and centrifuged at 13,000 rpm for 2 min at 4°C. Supernatants, representing the soluble material, were removed and then pellets were solubilized in 100 ml of solubilization buffer (50 mM Tris-HCl, pH 8.8, 5 mM EDTA, 1% SDS); DNA was sheared through a 22-g needle. Both soluble and insoluble materials were adjusted to 0.1% SDS before immunoprecipitation with specific antibodies as previously described (Le Bivic et al., 1989).

Sucrose Gradients

Sucrose gradient analysis of TX-100-insoluble residue was performed using previously published protocols (Brown and Rose, 1992; Zurzolo et al., 1994). Briefly, cells were grown to confluence in 100-mm dishes, labeled for 30 min with 500 mCi/ml of [³⁵S]met-cys, and then incubated in chase medium for 3 h. Monolayers were then rinsed in PBS CM and lysed for 20 min in TNE/TX-100 buffer on ice. Lysates were scraped from the dish, brought to 40% sucrose, and then placed at the bottom of a centrifuge tube. A linear sucrose gradient (5–35% in TNE) was layered on top of the lysates and then the samples were centrifuged at 39,000 rpm for 18–20 h in a rotor (model SW41; Beckman Instrs., Fullerton, CA). 1-ml fractions were harvested from the top of the gradient. Immunoprecipitation of gD1-DAF and other antigens was performed on the different fractions, after bringing them to ~20% sucrose and 1% TX-100. Samples were solubilized in Laemmli buffer and either boiled for 5 min, or left at 25°C for 30 min before running on SDS-PAGE, and were then analyzed by autoradiography.

Immunofluorescence and Electron Microscopy

Cells grown on coverslips to confluence were processed for immunofluorescence as described (Zurzolo et al., 1993). For EM experiments, cells were washed three times with PBS pH 7.4, containing 2.7 mM KCl, 1 mM CaCl₂, and 1 mM MgCl₂, and then fixed for 30 min at room temperature with 2.5% glutaraldehyde, 0.1% tannic acid in 0.1 M cacodylate buffer, pH 7.4. Cells were then rinsed three times in 0.1 M cacodylate buffer and postfixed in 1% osmium tetroxide in 0.1 M cacodylate buffer for 30–60 min at room temperature. Cells were further stained en bloc with 3% uranyl acetate in 50% ethanol for 20 min, dehydrated through graded ethanol, and finally embedded in Epon 812 (Polysciences, Inc., Warrington, PA). Thin sections were cut parallel to the plane of the culture on a microtome (model MT 5000; Sorvall, Inc., Newtown, CT) and then stained with 1.5% uranyl acetate and 0.1% lead citrate (Venable et al., 1965). For the immunogold localization of gD1-DAF, *cav1*-FRT cells grown to subconfluence on coverslips were incubated on ice with the monoclonal antibody anti-gD1-DAF for 1 h. After three washes in PBS, bound antibody was detected with goat anti-mouse IgG 10-nm gold conjugates. After three washes in PBS, the cells were processed as described above through to dehydration in ethanol. In 70% ethanol, cells were scraped from the coverslips with a razor blade and then the pellets were collected in a microfuge tube before embedding in Epon 812. Specimens were examined and photographed in either a 100 C X II (JEOL USA, Inc., Peabody, MA) or electron microscope (model 400T; Philips Electron Optics, Eindhoven, The Netherlands).

Results

Transfection of gD1-DAF and *cav1* in FRT Cells

We have previously shown that unlike MDCK cells (Lisanti et al., 1989), FRT cells sort gD1-DAF, a fusion protein between the ectodomain of the herpes simplex virus glycoprotein gD1 and the GPI-attachment signal from decay accelerating factor (DAF), to the basolateral membrane (Zurzolo et al., 1993) and fail to incorporate it into TIFF (Zurzolo et al., 1994). Because FRT cells do not express caveolin, a cholesterol binding protein, the possibility was raised that caveolin may be required for both association

of GPI-anchored proteins with TIFF and for targeting of GPI-anchored proteins to the apical surface (Dupree et al., 1993; Zurzolo et al., 1994).

To determine whether caveolin was involved in either the apical sorting of gD1-DAF or in its clustering with GSLs, we stably transfected FRT cells with a cDNA encoding the *cav1* protein. After initial attempts to transfect *cav1* into FRT cells already expressing gD1-DAF failed, we simultaneously transfected a plasmid containing the gD1-DAF gene under control of the RSV promoter (Lisanti et al., 1989), and then a plasmid containing the *cav1* coding sequence fused to the cytomegalovirus (CMV) promoter and the gene conferring resistance to neomycin (G418). By selection with G418, we isolated different clones expressing both proteins. Among many clones heterogeneous in their expression of caveolin and gD1-DAF proteins, as visualized by double immunofluorescence experiments (data not shown), we selected two clones (FRTc1 and FRTc2) that displayed a homogeneous distribution of both markers within all cells (Fig. 1, A and B). Both clones displayed caveolin as a punctate pattern at the plasma membrane and within the Golgi apparatus (Fig. 1 A). gD1-DAF was similarly enriched at the plasma membrane, albeit with a different, more diffuse, pattern (Fig. 1 B), but was also found intracellularly, as previously shown (Zurzolo et al., 1993).

*gD1-DAF Is Sorted to the Basolateral Membrane in *cav1*-transfected FRT Cells*

The immunofluorescence experiments demonstrated a characteristic ring-like basolateral distribution of surface gD1-DAF in *cav1*-FRT cells, identical to the localization we had previously observed in nontransfected cells (Zurzolo et al., 1993). To quantify this distribution, we performed a domain selective-biotinylation assay with both clones expressing caveolin, and with nontransfected cells for comparison. In agreement with the distribution observed by immunofluorescence, we found that gD1-DAF was basolaterally localized in both *cav1* expressing clones and in the wild-type cells (Fig. 2 A). In all cells we found that at steady state, 90–95% of the total surface protein was localized on the basolateral membrane. Furthermore, immunoprecipitation experiments demonstrated that the levels of *cav1* in clone 1 and clone 2 were 90 and 60%, respectively, of the levels found in MDCK cells (Fig. 2 B).

As additional controls, we also examined the plasma membrane distribution of several endogenous apical (DPPIV) and basolateral (35–40-kD Ag, NaK-ATPase) antigens (Zurzolo et al., 1992, Zurzolo and Rodriguez-Boulan, 1993) in the caveolin-transfected cells by immunofluorescence and surface biotinylation. The polarity of these markers was unchanged compared with nontransfected cells (data not shown). These data clearly demonstrated that *cav1* expression did not revert the basolateral sorting of gD1-DAF in FRT cells.

gD1-DAF Is Excluded from TIFF in FRT Cells Expressing Cav1

In MDCK cells, GPI-anchored proteins are incorporated into TX-100-insoluble aggregates, presumably reflecting their association with GSLs in the Golgi complex (Brown

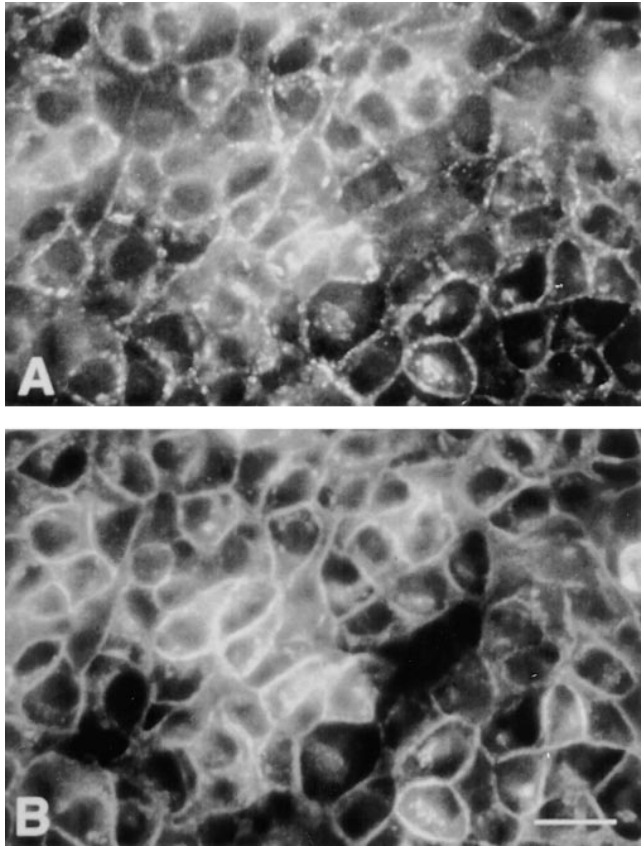


Figure 1. Localization by double immunofluorescence of *cav1* and gD1-DAF in transfected FRT cells. A stable FRT clonal line expressing *cav1* and gD1-DAF was grown to confluence on glass coverslips. Cells were fixed with paraformaldehyde and permeabilized with PBS CM containing 0.2% gelatin and 0.075% saponin, and then stained using a polyclonal antibody against caveolin (A) and a monoclonal antibody against gD1-DAF (B). Primary antibodies were visualized using anti-mouse TRITC-conjugated and anti-rabbit FITC-conjugated antibodies. Cav1 gave a punctate staining localized both at the plasma membrane and, less intensely, at the Golgi apparatus, whereas gD1-DAF was enriched mainly at the basolateral surface. Bar, 50 μ m.

and Rose, 1992). In apparent agreement with the idea that this association may be required for their apical sorting (Van Meer and Simons, 1988; Lisanti and Rodriguez-Boulan, 1990), we previously demonstrated that basolaterally sorted gD1-DAF fails to be incorporated into TIFFF in FRT cells, whereas it is apically sorted and becomes detergent insoluble in MDCK cells (Zurzolo et al., 1994). To determine whether transfection of *cav1* promotes clustering of gD1-DAF with GSLs, we performed pulse-chase experiments in the two FRT clones stably expressing *cav1*, and then determined whether gD1-DAF was incorporated into the TX-100-insoluble fraction. We found that in both caveolin expressing clones, gD1-DAF was mainly soluble in TX-100 at all times of chase (Fig. 3), exactly as previously shown in nontransfected cells (Zurzolo et al., 1994).

We then analyzed the TX-100-insoluble fractions by sucrose density-gradient centrifugation and immunoprecipitation of gD1-DAF from all fractions. In the caveolin-expressing FRT clones, neither the mature nor immature

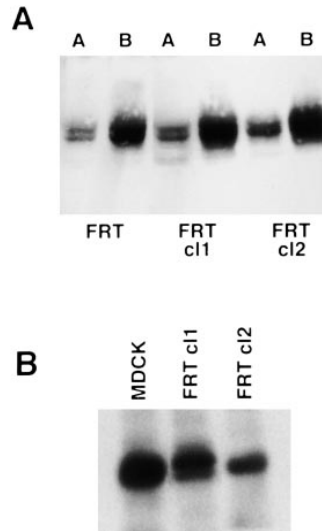


Figure 2. Surface distribution of gD1-DAF in *cav1*-transfected and wild-type FRT cells. FRT cells expressing gD1-DAF or both gD1-DAF and caveolin (*cl1* and *cl2*) were grown on filters for 5 d and then labeled with [³⁵S]met-cys overnight. (A) Surface-expressed gD1-DAF was selectively biotinylated from the apical (A) or basolateral (B) side, extracted, and immunoprecipitated with a specific monoclonal antibody, and then the biotinylated fraction was subsequently precipitated with streptavidin beads. Immunoprecipitated proteins were visualized by 10% SDS-PAGE and autoradiography. Note that gD1-DAF was enriched on the basolateral surface (~95% of total membrane proteins) both in transfected and nontransfected cells. (B) The quantity of caveolin synthesized by the two FRT clones was compared to the amounts present in MDCK cells by immunoprecipitation of [³⁵S]met-cys cells with a polyclonal antibody against caveolin.

forms of gD1-DAF floated to the top of the gradient, as was shown in MDCK cells (Zurzolo et al., 1994); instead, both forms were enriched in fractions 8–12 (40% sucrose) at the bottom of the gradient, as expected for soluble proteins (Fig. 4). The small amount of gD1-DAF floating to TIFFF in clone 2 was reproducible and corresponded to the small quantity of insoluble gD1-DAF found in this clone (Fig. 3). This result was not related to different levels of caveolin expressed by the two clones, but is simply a consequence of clonal variation among FRT cells. In fact, similar amounts of insoluble and floating gD1-DAF were found in the nontransfected FRT population lacking caveolin, as was previously reported (Zurzolo et al., 1994). These experiments indicated that transfection of *cav1* was not able to reverse the inability of gD1-DAF to partition with TIFFF in FRT cells.

forms of gD1-DAF floated to the top of the gradient, as was shown in MDCK cells (Zurzolo et al., 1994); instead, both forms were enriched in fractions 8–12 (40% sucrose) at the bottom of the gradient, as expected for soluble proteins (Fig. 4). The small amount of gD1-DAF floating to TIFFF in clone 2 was reproducible and corresponded to the small quantity of insoluble gD1-DAF found in this clone (Fig. 3). This result was not related to different levels of caveolin expressed by the two clones, but is simply a consequence of clonal variation among FRT cells. In fact, similar amounts of insoluble and floating gD1-DAF were found in the nontransfected FRT population lacking caveolin, as was previously reported (Zurzolo et al., 1994). These experiments indicated that transfection of *cav1* was not able to reverse the inability of gD1-DAF to partition with TIFFF in FRT cells.

Caveolin Forms Oligomers and Associates with TIFFF in Transfected FRT Cells

To rule out the possibility that the lack of effect of *cav1* on the partitioning of gD1-DAF in TIFFF was because of the inability of caveolin itself to localize in the insoluble fractions in the transfected FRT clones, we performed a sucrose density-gradient purification of TIFFF followed by immunoprecipitation of the different fractions with an anticaveolin antibody. We found that a considerable amount of the protein (20–30% of the total) was found in the TIFFF (fractions 5, 6, and 7 corresponding to 20–25% sucrose; Fig. 5, top). As a control we also followed the migration of caveolin to the TIFFF in MDCK cells. In this cell line, a similar amount of the protein migrated to the lighter fractions 5, 6, and 7 of the gradient (Fig. 5, bottom). Therefore, the lack of effect of caveolin on GPI-proteins/GSLs cluster formation was not because of the inability of caveolin itself to localize in the TIFFF.

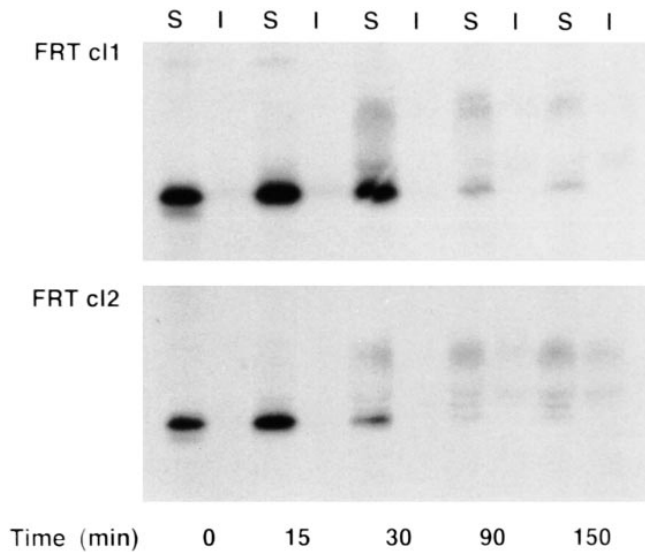


Figure 3. Pulse-chase analysis of gD1-DAF solubility in TX-100 in FRT cells expressing *cav1*. FRT cells stably expressing gD1-DAF and caveolin (*c11* and *c12*) were grown to confluence and then pulsed for 5 min with [³⁵S] met-cys, followed by incubation in chase medium for the indicated times. After extraction in TNE-1% TX-100 buffer at 4°C, both the soluble (*S*, supernatant) and insoluble (*I*, pellet) fractions were collected after centrifugation, and then gD1-DAF was subsequently immunoprecipitated and analyzed by SDS-PAGE and fluorography. In both clones, gD1-DAF is mostly soluble at all chase times during its transport to the cell surface. The small amount of insoluble gD1-DAF found in clone 2 is likely to be a result of clonal variation. In fact, a similar amount of insoluble gD1-DAF was also found in non-transfected cells (Zurzolo et al., 1994).

These experiments also revealed that similar high molecular weight complexes resistant to boiling were found in the two cell lines. To better resolve these complexes on the gel and to follow their migration on the gradients, we performed a similar experiment in the two cell lines without boiling the samples. These experiments clearly showed that transfected caveolin in FRT cells formed oligomers of molecular weights of ~350, 300, and 200 kD, as well as 45-kD dimers (Fig. 6, *top*), similar to that formed by endogenous caveolin in MDCK cells (Fig. 6, *bottom*) as previously shown (Monier et al., 1995; Sargiacomo et al., 1995). Furthermore, these oligomers appeared to migrate to TIFF in both cell lines in similar amounts as the monomer (compare Figs. 5 and 6, *top* and *bottom*).

Endogenous GPI-anchored Proteins Distribute Basolaterally in Wild-Type and *cav1*-transfected FRT Cells

To determine whether caveolin transfection affected the polarity of endogenous GPI-anchored proteins in FRT cells, we studied their steady-state localization using domain-selective biotinylation in combination with partition into Triton X-114 and treatment with phospholipase C (Lisanti et al., 1988). As shown in Fig. 7, the majority of endogenous GPI-anchored proteins were basolaterally localized in the *cav1*-expressing cells. This result was identical to that obtained in nontransfected cells (Zurzolo et al., 1993). Therefore, caveolin expression appears to have no

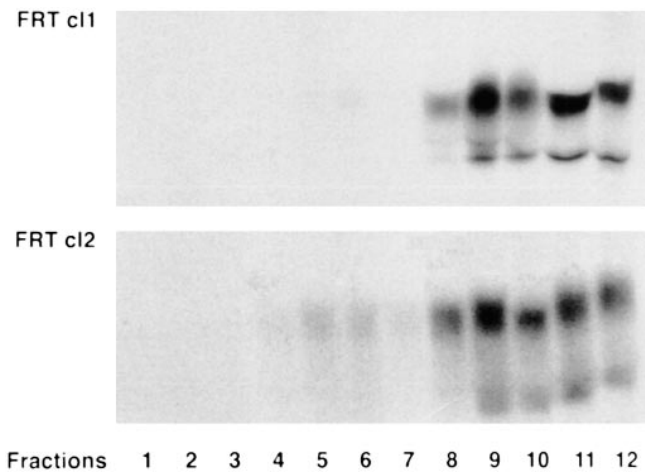


Figure 4. Purification of gD1-DAF-enriched fractions on sucrose density gradients. FRT cells expressing gD1-DAF and caveolin (*c11* and *c12*) were labeled with [³⁵S]met-cys for 30 min and then chased for 3 h. Cells were lysed in TNE/TX-100 buffer and then run through a linear 5–40% sucrose gradient. Fractions of 1 ml were collected from top to bottom after centrifugation to equilibrium, and then gD1-DAF was immunoprecipitated from all fractions. In both clones, mature and immature gD1-DAF forms are almost exclusively restricted to the bottom fractions.

effect on GPI-anchored protein distribution, which remains predominantly basolateral, exactly as in FRT cells not expressing caveolin.

***Cav1* Promotes Formation of Caveolae in Transfected FRT Cells**

Previous experiments showed that transient expression of VIP21/*cav1* using a Semliki Forest virus vector in lymphocytes lacking caveolin promoted the formation of plasmalemmal caveolae (Fra et al., 1995). Furthermore, it was suggested that the formation of large caveolin oligomers might be required for caveolar assembly (Parton and Simons, 1995; Sargiacomo et al., 1995). To definitively address the role of caveolin in caveolar formation, we assayed for the presence of caveolae in the stably transfected and nontransfected FRT cells. Using 0.1% tannic acid to enhance visualization of caveolar invaginations by EM (Palade and Bruns, 1968), we observed that wild-type FRT cells have no plasmalemmal caveolae (Fig. 8, *A* and *B*). In contrast, FRT cells expressing caveolin displayed large numbers of normal flask-shaped caveolae (Palade and Bruns, 1968), frequently organized into characteristic racemose clusters (Fig. 8, *C–E*). These data showed that *cav1* was necessary and sufficient to promote efficient caveolae formation in FRT cells.

To determine whether gD1-DAF was able to localize in these caveolae at the surface of the transfected FRT cells, we performed an immuno-EM localization of gD1-DAF after cross-linking with antibodies. We found that gD1-DAF was distributed upon the entire surface of transfected FRT cells, and that it was able to cluster in caveolae upon antibody cross-linking (Fig. 9, *A–D*) as was previously shown in other cell lines (Mayor et al., 1994; Parton et al., 1994; Mayor and Maxfield 1995). These experiments indicated that in FRT cells, the newly formed caveolae are

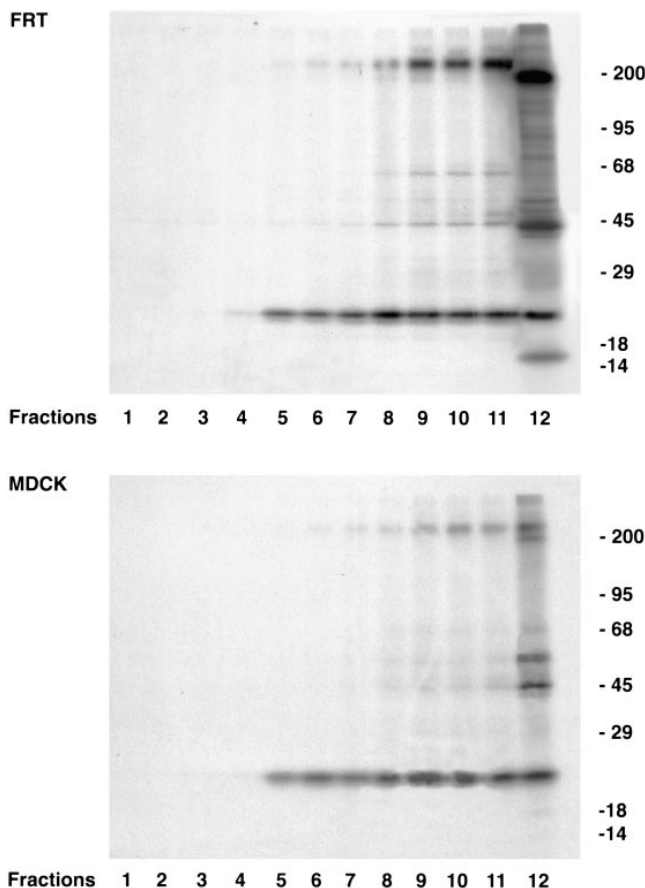


Figure 5. Purification of caveolin-enriched fractions on sucrose density gradients in MDCK and *cav1*-transfected FRT cells (I). *cav1*-FRT and MDCK cells were labeled with [³⁵S]met-cys for 30 min and then chased for 3 h. Cells were lysed in TNE/TX-100 buffer and then run through a linear 5–40% sucrose gradient. Fractions of 1 ml were collected from top to bottom after centrifugation to equilibrium, and then caveolin was immunoprecipitated from all fractions. After solubilization in Laemmli buffer and boiling for 5 min, the samples were run on a 6–15% acrylamide gradient SDS gel. Caveolin is present in both the soluble (9–12) and insoluble (5–7) fractions in both *cav1*-FRT and MDCK cells.

able to interact with GPI-anchored proteins and, together with our other data, suggest that *cav1* and caveolae are not involved in GPI-anchored protein trafficking.

Discussion

The raft hypothesis postulates that apically localized plasma membrane proteins laterally associate with GSLs into segregated microdomains as a prerequisite for sorting into apical transport vesicles in the TGN (Simons and Ikonen, 1997). The most frequently used method to identify these lipid microdomains and to follow the partitioning of a protein within them is to determine whether the lipids and the proteins are insoluble in certain nonionic detergents (TX-100, TX-114, CHAPS) and whether they cofloat into the lighter density region (TIFF or DIG) of sucrose density gradients (for review see Kurzchalia et al., 1995; Parton, 1996). Although different transmembrane

apical proteins show variable association with TIFFs according to this criterion, GSLs and GPI-anchored proteins appear to be consistently incorporated into TIFFs in different epithelial cells, where they are apically targeted (Lisanti and Rodriguez-Boulan, 1990; Brown and Rose, 1992; Mirre et al., 1996). From this perspective, GPI-anchored proteins appear to require GSL association for apical targeting. Our previously published data, showing the failure of FRT cells to target GPI-anchored proteins and GSLs apically and to incorporate GPI-anchored proteins into TIFF, provides additional support for this hypothesis (Zurzolo et al., 1993, 1994). Therefore, if GPI-anchored proteins are indeed cosorted, the question arises as to what is the mechanism that promotes their association in microdomains at the level of the TGN and then leads to their apical sorting.

Recent circumstantial evidence suggests that the caveolar coat protein caveolin might play a role in the clustering of GSLs and GPI-anchored proteins (Dupree et al., 1993; Sargiacomo et al., 1993; Zurzolo et al., 1994). Although TIFF exists in the absence of plasmalemmal caveolae, the lipid composition of caveolae is very similar to that of TIFF (Brown and Rose, 1992; Fra et al., 1995). Furthermore, it has been shown that caveolin, which is 90% enriched in plasma membrane caveolae, associates with TIFF (Sargiacomo et al., 1993; Kurzchalia et al., 1995). Although some controversy exists as to whether GPI-anchored proteins are enriched within caveolae (Rothberg et al., 1990; Anderson, 1993; Mayor et al., 1994), nonetheless, these proteins show affinity for caveolae after they have been cross-linked with antibodies. Finally, the presence of caveolin in the TGN and post-TGN vesicles (Kurzchalia et al., 1992), and the absence of caveolin in FRT cells, which exhibit defective apical targeting and clustering of GPI-anchored proteins, further underlines the need for studies that address the role of caveolin in intracellular sorting of proteins in the Golgi complex.

The approach we used in this report was to transfect the *cav1* gene into FRT cells to determine its effect on the sorting of GPI-anchored proteins and its association with TIFF. In two FRT clones stably expressing caveolin at levels comparable with MDCK cells, we observed that although caveolin typically associated with TIFF and formed large oligomers similar to those assembled in MDCK cells, gD1-DAF remained unable to cluster with GSLs that independently fractionated into TIFF, and was still sorted to the basolateral membrane, as in wild-type cells. Furthermore, no changes were detected in the distribution of endogenous GPI-anchored proteins, which remained mainly basolateral or nonpolar. Taken together, our data suggest that *cav1* does not mediate the association of GPI-anchored proteins with GSL-enriched microdomains in the Golgi complex, nor participates in apical sorting.

Another possible explanation for our results is that *cav1* is, for some reason, nonfunctional in FRT cells and, therefore, fails to carry out the functions that it performs normally in other cells. For example, FRT cells might not be able to perform a critical posttranslational processing modification of *cav1*, or might fail to form the oligomers observed in MDCK cells. To test this hypothesis, we studied the effect of *cav1* transfection on the assembly of plasma membrane caveolae. Indeed, we found that wild-

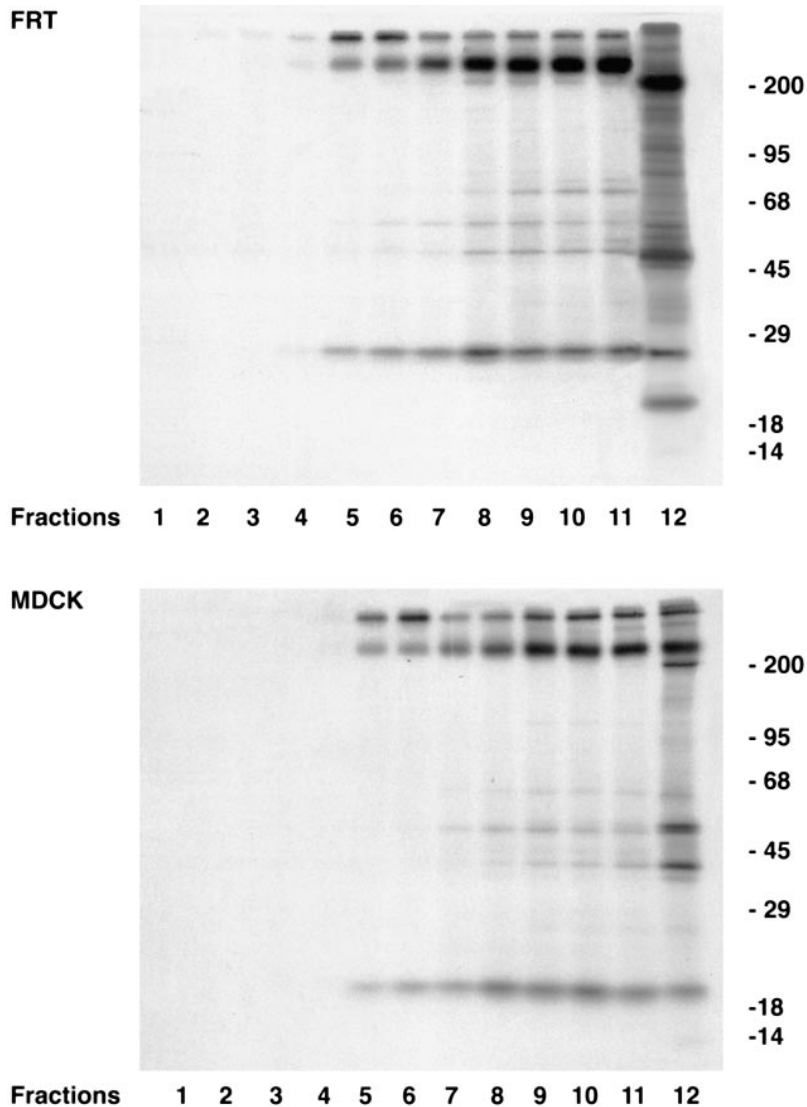


Figure 6. Purification of caveolin-enriched fractions on sucrose density gradients in MDCK and *cav1*-transfected FRT cells (II). *Cav1*-FRT and MDCK cells were treated as described in Fig. 5. 1-ml fractions from a 5–40% linear sucrose density gradient were immunoprecipitated using a polyclonal antibody against caveolin. Samples were lysed in Laemmli buffer and then left 30 min at 25°C before loading them on a 6–15% acrylamide gradient SDS gel. In both *cav1*-FRT and MDCK cells, caveolin forms oligomers of high molecular weight (~350, 300, and 200 kD), which are localized in the bottom fractions as well as within the lighter fractions of the gradients.

type FRT cells do not form caveolae, but, upon transfection with *cav1*, formed large numbers of normal flask-shaped caveolae. Our results confirm and extend previous experiments in which caveolin transfection was shown to be necessary and sufficient to promote the assembly of caveolae in lymphocytes (Fra et al., 1995). FRT caveolae were indistinguishable from the caveolae endogenously present in other epithelial and endothelial cells; they frequently showed a classical septum at the neck and often associated into racemose clusters of five or six units (Fig. 8) (Palade and Bruns, 1968). We also found that gD1-DAF clustered into these newly formed caveolae upon cross-linking with antibodies. Furthermore, *cav1* transfected into FRT cells forms high molecular weight oligomers as in cells that form caveolae, such as MDCK cells. Therefore, our results show that both *cav1* and caveolae are functional in FRT cells, as judged by (a) the ability of *cav1* to oligomerize and promote caveolar assembly, and (b) by the capacity of these organelles to interact with GPI-anchored proteins. This is the first report of caveolar assembly in cells permanently transfected with caveolin.

Although our data indicate that *cav1* is functional and

sufficient to promote the assembly of caveolae in FRT cells, they do not exclude the possibility that FRT cells lack additional factor(s) required for GPI-anchored protein clustering with GSLs, enriched microdomains, and/or apical sorting. For example, GPI-anchored proteins might have different intrinsic properties in FRT cells that prevent their clustering with GSLs. Alternatively, FRT cells might lack a clustering molecule that would be involved in partitioning GPI-anchored proteins into GSL clusters. However, some data already present in the literature do not favor a role for caveolin in these processes (Gorodinsky and Harris, 1995; Kurzchalia et al., 1995; Mirre et al., 1996). Most importantly, CaCo₂ cells lack caveolin and are, nonetheless, able to form TX-100-insoluble GSLs/GPI-protein-enriched microdomains, and sort them to the apical plasma membrane (Mirre et al., 1996).

Because we did not check whether FRT cells also lack caveolin2 (Parton, 1996; Scherer et al., 1996), a possibility remains that this isoform of caveolin could have some role in the apical sorting of GPI-anchored proteins. However, considering that such a role was proposed originally for *cav1*, which was found to be enriched in the TGN and

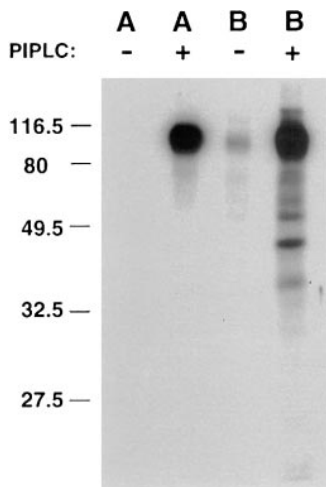


Figure 7. Steady-state distribution of endogenous GPI-anchored proteins in *cav1*-transfected FRT cells. FRT cells expressing *cav1*, grown to confluence on polycarbonate filters for 5 or 6 d, were subjected to domain-specific biotinylation from the apical (lanes *A*⁻, *A*⁺) or from the basolateral (lanes *B*⁻, *B*⁺) surface of the monolayer. After extraction with Triton X-114 and phase separation, detergent phases were incubated in the presence (lanes *A*⁺, *B*⁺) or in the absence (lanes *A*⁻, *B*⁻) of GPI-specific phospholipase C (6 U/ml). After phase separation, biotinylated proteins in the aqueous phase were TCA precipitated, subjected to SDS-PAGE, and then visualized by Western blotting using ¹²⁵I-streptavidin. Molecular masses (top to bottom, are 116.5, 80, 49.5, 32.5, and 27.5 kD). In *cav1*-FRT cells, one GPI-anchored protein is not polarized, whereas the rest are found on the basolateral membrane, as was previously shown in nontransfected FRT cells (Zurzolo et al., 1993).

post-TGN sorting vesicles (Dupree et al., 1993; Kurzchalia et al., 1992), and considering that caveolin2 appears to be targeted largely to the basolateral plasma membrane in MDCK cells (Scheiffele et al., 1998), we believe this scenario is unlikely.

The data reported here support the hypothesis that caveolin oligomerization is the basis of caveolar coat assembly (Anderson, 1993; Fra et al., 1995; Monier et al., 1995) and clearly demonstrate that *cav1* is necessary and sufficient to promote formation of these characteristic plasma membrane invaginations. Furthermore, because we found similar levels of TX-100-insoluble GSLs in FRT cells expressing or not expressing *cav1* and caveolae, our data definitively rule out the suggested identity between caveolae and detergent-insoluble microdomains, and do not support a role for caveolae as carrier vesicles for the transport of GPI-anchored proteins to the apical plasma membrane.

An alternative model is that clustering with GSLs is indeed a prerequisite for apical sorting of GPI-anchored proteins, and that caveolin and caveolae are not involved in these events. Although it is not yet clear whether incorporation of a protein in these rafts would be sufficient for apical sorting, there could be different mechanisms mediating the association of GPI-anchored proteins with GSLs rafts. One could hypothesize that MDCK and other epithelial cells that sort GPI-anchored proteins to the apical surface possess a clustering factor, such as was originally suggested for caveolin, that could also be recognized as an apical targeting signal. An equivalent function could be performed by the membrane-spanning domains of apical transmembrane proteins (Kundu et al., 1996). Additionally, the ectodomain may also play a role in apical sorting since it has been shown that most of the ectodomains of GPI-anchored proteins are secreted selectively into the apical medium (Brown et al., 1989; Lisanti et al., 1989; Powell et al., 1991). Further experiments will be necessary

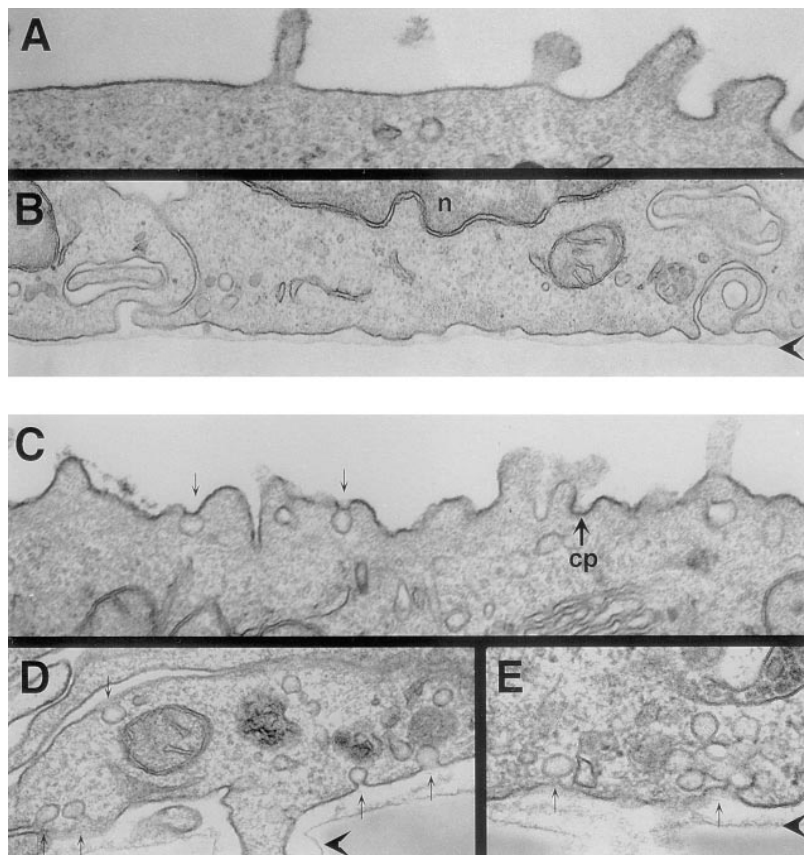


Figure 8. Electron micrographs of wild-type and caveolin-expressing FRT cells. *Cav1*-transfected and nontransfected FRT cells were grown on filters for 5 d, and then fixed and treated for EM as described in Materials and Methods. Apical side (A) and basal side (B) of nontransfected FRT cells. Note the absence of plasmalemmal caveolae on both surfaces. FRT cells transfected with *cav1* contain caveolae both on the apical (C) and basolateral membranes (D and E) characterized as coat-free flask-shaped plasmalemmal invaginations with the diaphragm at the neck (small arrows). Note on the basal side (E) the characteristic cluster of caveolae into racemose structures (small arrow). *cp* indicates coated pit; *n* indicates nucleus; arrowheads show the edge of the filter.

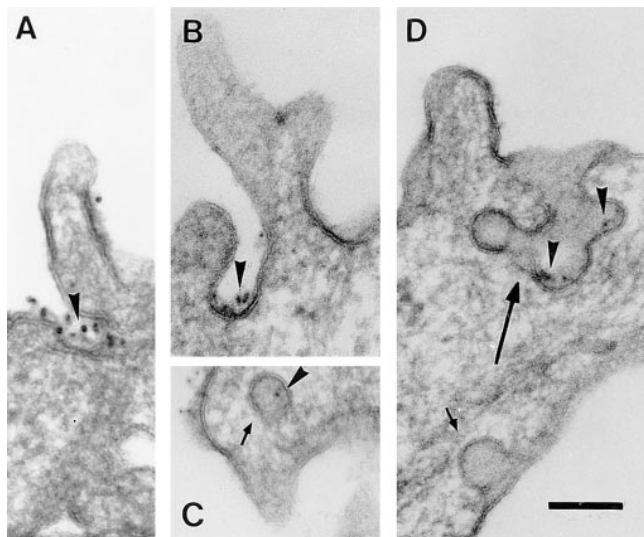


Figure 9. Immunogold localization of gD1-DAF on the surface of caveolin-expressing FRT cells. *Cav1*-FRT cells were grown to subconfluence on coverslips, incubated with an anti-gD1-DAF monoclonal antibody on ice for 1 h and, after washing in PBS, with a secondary antibody conjugated with 10-nm colloidal gold on ice for 1 h. After fixation, cells were dehydrated through graded ethanol and were scraped from the coverslips in 70% ethanol. The pellets were then processed as described in Materials and Methods. *A–D* show different sections of apical and basolateral plasma membranes of *cav1*-FRT cells that contain gD1-DAF clustered in newly formed (*A* and *B*) or classical flask-shaped caveolae (*C* and *D*; small arrows). A racemose cluster of caveolae containing gD1-DAF is shown on the apical surface (*D*; large arrow). Arrowheads indicate the gold particles bound to the anti-gD1-DAF antibody. Bar, 100 nm.

to discriminate among these possibilities. Since the sorting machinery seems to be conserved also in nonpolarized cells (Musch et al., 1996; Yoshimori et al., 1996), we believe that the use of *in vitro* assays, together with comparative analyses between different epithelial cells displaying different sorting profiles of GPI-anchored proteins and GSLs, will help to address these possibilities.

We would like to thank P. Dupree and R. Anderson for the caveolin cDNA and I. Caras for the gD1-DAF cDNA. We also thank L. Cohen-Gould (Cornell University Medical College) for efficient technical assistance with the electron microscopy, and Mario Belardone (Naples University, Naples, Italy) for photographic reproductions.

Work in the Zurzolo lab was supported by Ministero Università e Ricerca Scientifica e Tecnologica. Work in the Rodriguez-Boulant lab was supported by a National Institutes of Health grant (GM41771).

Received for publication 14 July 1997 and in revised form 1 December 1997.

References

Ali, N., and W.H. Evans. 1990. Priority targeting of glycosyl-phosphatidylinositol-anchored proteins to the bile canalicular (apical) plasma membrane of hepatocytes. *Biochem. J.* 271:193–199.

Anderson, R.G.W. 1993. Plasmalemmal caveolae and GPI-anchored membrane proteins. *Curr. Opin. Cell Biol.* 5:647–652.

Brown, D.A., B. Crise, and J.K. Rose. 1989. Mechanism of membrane anchoring affects polarized expression of two proteins in MDCK cells. *Science*. 245:1499–1501.

Brown, D.A., and J.K. Rose. 1992. Sorting of GPI-anchored proteins to glycolipid-enriched membrane subdomains during transport to the apical cell

surface. *Cell*. 68:533–544.

Cross, G.A.M. 1987. Eukaryotic protein modification and membrane attachment via phosphatidylinositol. *Cell*. 48:179–181.

Doering, T.L., W.J. Masterson, P.T. Englund, and G.W. Hart. 1990. Biosynthesis of glycosylphosphatidylinositol membrane anchors. *J. Biol. Chem.* 265:611–614.

Drubin, D.G., and W.J. Nelson. 1996. Origins of cell polarity. *Science*. 84:335–344.

Dupree, P., R.G. Parton, G. Raposo, T.V. Kurzchalia, and K. Simons. 1993. Caveolae and sorting in Trans Golgi Network of epithelial cells. *EMBO (Eur. Mol. Biol. Organ.) J.* 12:1597–1605.

Eaton, S., and K. Simons. 1995. Apical, basal, and lateral cues for epithelial polarization. *Cell*. 82:5–8.

Englund, P.T. 1993. The structure and biosynthesis of glycosyl phosphatidylinositol protein anchors. *Annu. Rev. Biochem.* 62:121–138.

Ferguson, M.A.J., and A.F. Williams. 1988. Cell-surface anchoring of proteins via glycosyl-phosphatidyl structures. *Annu. Rev. Biochem.* 57:285–320.

Fra, A.M., E. Williamson, K. Simons, and R.G. Parton. 1994. Detergent-insoluble glycolipid microdomains in lymphocytes in the absence of caveolae. *J. Biol. Chem.* 269:30745–30748.

Fra, A.M., E. Williamson, K. Simons, and R.G. Parton. 1995. De novo formation of caveolae in lymphocytes by expression of VIP21-caveolin. *Proc. Natl. Acad. Sci. USA*. 92:8655–8659.

Garcia, M., C. Mirre, A. Quaroni, H. Reggio, and A. Le Bivic. 1993. GPI anchored proteins associate to form microdomains during their intracellular transport in CaCo2 cells. *J. Cell Sci.* 104:1281–1290.

Gorodinsky, A., and D.A. Harris. 1995. Glycolipid-anchored proteins in neuroblastoma cells form detergent-resistant complexes without caveolin. *J. Cell Biol.* 129:619–627.

Hannan, L.A., M.P. Lisanti, E. Rodriguez-Boulant, and M. Edidin. 1993. Correctly sorted molecules of a GPI-anchored protein are clustered and immobile when they arrive at the apical surface of MDCK cells. *J. Cell Biol.* 120:353–358.

Kundu, A., R.T. Avalos, C.M. Sanderson, and D.P. Nayak. 1996. Transmembrane domain of influenza virus neuraminidase, a type II protein, possesses an apical sorting signal in polarized MDCK cells. *J. Virol.* 70:6508–6515.

Kurzchalia, T.V., P. Dupree, R.G. Parton, R. Kellner, H. Virta, M. Lehnert, and K. Simons. 1992. VIP 21, a 21-kD membrane protein is an integral component of trans-Golgi network-derived transport vesicles. *J. Cell Biol.* 118:1003–1014.

Kurzchalia, T.V., E. Hartmann, and P. Dupree. 1995. Guilt by insolubility—does a protein's detergent-insolubility reflect a caveolar location? *Trends Cell Biol.* 5:187–189.

Laemmli, U.K. 1970. Cleavage of structural proteins during the assembly of the head of the bacteriophage T4. *Nature*. 227:680–685.

Le Bivic, A., F.X. Real, and E. Rodriguez-Boulant. 1989. Vectorial targeting of apical and basolateral plasma membrane protein in a human adenocarcinoma epithelial cells. *Proc. Natl. Acad. Sci. USA*. 86:9313–9317.

Le Gall, A.H., C. Yeman, A. Muesch, and E. Rodriguez-Boulant. 1995. Epithelial cell polarity: new perspectives. *Semin-Nephrol.* 15:272–284.

Lisanti, M.P., M. Sargiacomo, L. Graeve, A. Saltiel, and E. Rodriguez-Boulant. 1988. Polarized apical distribution of glycosylphosphatidyl inositol anchored proteins in a renal epithelial line. *Proc. Natl. Acad. Sci. USA*. 85:9557–9561.

Lisanti, M.P., I.W. Caras, M.A. Davitz, and E. Rodriguez-Boulant. 1989. A glycosphingolipid membrane anchor acts as an apical targeting signal in polarized epithelial cells. *J. Cell Biol.* 109:2145–2156.

Lisanti, M., and E. Rodriguez-Boulant. 1990. Glycosphingolipid membrane anchoring provides clues to the mechanism of protein sorting in polarized epithelial cells. *Trends Biochem. Sci.* 15:113–118.

Lisanti, M.P., E. Rodriguez Boulant, and A.R. Saltiel. 1990. Preferred apical distribution of glycosyl-phosphatidylinositol (GPI) anchored proteins: a highly conserved feature of the polarized epithelial cell phenotype. *J. Membr. Biol.* 113:155–167.

Low, M. 1989. The glycosyl-phosphatidylinositol anchor of membrane proteins. *Biochim. Biophys. Acta*. 988:427–454.

Low, M.G., and A.R. Saltiel. 1988. Structural and functional roles of glycosylphosphatidylinositol in membranes. *Science*. 239:268–275.

Matter, K., and I. Mellman. 1994. Mechanisms of cell polarity: sorting and transport in epithelial cells. *Curr. Opin. Cell Biol.* 6:545–554.

Mayor, S., and F.R. Maxfield. 1995. Insolubility and redistribution of GPI-anchored proteins at the cell surface after detergent treatment. *Mol. Biol. Cell*. 6:929–944.

Mayor, S., K.G. Rothberg, and F.R. Maxfield. 1994. Sequestration of GPI-anchored proteins in caveolae triggered by cross-linking. *Science*. 264:1948–1951.

McConville, M.J., and M.A.J. Ferguson. 1993. The structure, biosynthesis, and function of glycosylated phosphatidylinositols in the parasitic protozoa and higher eukaryotes. *Biochem. J.* 29:305–324.

Mirre, C., L. Monlauzer, M. Garcia, M.-H. Delgrossi, and A. Le Bivic. 1996. Detergent resistant membrane microdomains from Caco-2 cells do not contain caveolin. *Am. Physiol. Soc.* 271:C887–C894.

Monier, S., R.G. Parton, F. Vogel, A. Henske, and T.V. Kurzchalia. 1995. VIP21-caveolin, a membrane protein constituent of the caveolar coat, forms high molecular mass oligomers *in vivo* and *in vitro*. *Mol. Biol. Cell*. 6:911–927.

Mostov, K.E., G. Apodaca, B. Aroeti, and C. Okamoto. 1992. Plasma membrane protein sorting in polarized epithelial cells. *J. Cell Biol.* 116:577–583.

Muratata, M., J. Peranen, R. Schreiner, F. Wieland, T.V. Kurzchalia, and K. Si-

- mons. 1995. VIP21/caveolin is a cholesterol-binding protein. *Proc. Natl. Acad. Sci. USA*. 92:10339–10343.
- Musch, A., H. Xu, D. Shields, and E. Rodriguez-Boulau. 1996. Transport of VSV G protein to the cell surface is signal mediated in polarized and nonpolarized cells. *J. Cell Biol.* 133:543–558.
- Nitsch, L., D. Tramontano, N. Quarto, S. Bonatti, and F.S. Ambesi-Impimbato. 1985. Morphological and functional polarity of an epithelial thyroid cell line. *Eur. J. Cell Biol.* 38:57–66.
- Palade, G.E., and R.R. Bruns. 1968. Structural modulations of plasmalemmal vesicles. *J. Cell Biol.* 37:633–649.
- Parton, R.G. 1996. Caveolae and caveolins. *Curr. Opin. Cell Biol.* 8:542–548.
- Parton, R.G., and K. Simons. 1995. Digging into caveolae. *Science*. 269:1398–1399.
- Parton, R.G., B. Jøggerst, and K. Simons. 1994. Regulated internalization of caveolae. *J. Cell Biol.* 127:1199–1215.
- Powell, S.K., M.P. Lisanti, and E. Rodriguez-Boulau. 1991. Thy-1 expresses two signals for apical localization in epithelial cells. *Am. Physiol. Soc.* 260:C715–C720.
- Rodriguez-Boulau, E., and S.K. Powell. 1992. Polarity of epithelial and neuronal cells. *Annu. Rev. Cell Biol.* 8:395–427.
- Rothberg, K.G., Y.-S. Ying, J.F. Kolhouse, B.A. Kamen, and R.G.W. Anderson. 1990. The glycosphingolipid-linked folate receptor internalizes folate without entering the clathrin-coated pit endocytic pathway. *J. Cell Biol.* 110:637–649.
- Rothberg, K.G., J.K. Heuser, W.C. Donzell, Y.-S. Ying, J.R. Glenney, and R.G.W. Anderson. 1992. Caveolin, a protein component of caveole membrane coats. *Cell*. 68:673–682.
- Sargiacomo, M., M. Lisanti, L. Greve, A. Le Bivic, and E. Rodriguez-Boulau. 1989. Integral and peripheral protein composition of the apical and basolateral membrane domains in MDCK cells. *J. Membr. Biol.* 107:277–286.
- Sargiacomo, M., M. Sudol, Z. Tang, and M.P. Lisanti. 1993. Signal transducing molecules and GPI-linked proteins form a caveolin-rich insoluble complex in MDCK cells. *J. Cell Biol.* 122:789–807.
- Sargiacomo, M., P.E. Scherer, Z. Tang, E. Kuebler, K.S. Song, M. Sanders, and M.P. Lisanti. 1995. Oligomeric structure of caveolin: implications for caveolae membrane organization. *Proc. Natl. Acad. Sci. USA*. 92:9407–9411.
- Scheiffele, P., P. Verkade, A.M. Fra, H. Vicia, K. Simons, and E. Ikonen. 1998. Caveolin-1 and -2 in the exocytic pathway of MDCK cells. *J. Cell Biol.* In press.
- Scherer, P.E., T. Okamoto, M. Chun, I. Nishimoto, H.F. Lodish, and M.P. Lisanti. 1996. Identification, sequence, and expression of caveolin-2 defines a caveolin gene family. *Proc. Natl. Acad. Sci. USA*. 93:131–135.
- Schnitzer, J.E., P. Oh, B.S. Jacobson, and A.M. Dvorak. 1995a. Caveolae from luminal plasmalemma of rat lung endothelium: microdomains enriched in caveolin, Ca²⁺-ATPase, and inositol triphosphate receptor. *Proc. Natl. Acad. Sci. USA*. 92:1759–1763.
- Schnitzer, J.E., D.P. McIntosh, A.M. Dvorak, J. Liu, and P. Oh. 1995b. Separation of caveolae from associated microdomains of GPI-anchored proteins. *Science*. 269:1435–1439.
- Schroeder, R., E. London, and D. Brown. 1994. Interactions between saturated acyl chains confer detergent resistance on lipids and glycosylphosphatidylinositol (GPI)-anchored proteins: GPI-anchored proteins in liposomes and cells show similar behavior. *Proc. Natl. Acad. Sci. USA*. 91:12130–12134.
- Simons, K., and E. Ikonen. 1997. Functional rafts in cell membranes. *Nature*. 387:569–572.
- Skibbens, J.E., M.G. Roth, and K.S. Matlin. 1989. Differential extractability of influenza virus Hemagglutinin during intracellular transport in polarized epithelial cells and nonpolar fibroblasts. *J. Cell Biol.* 108:821–832.
- Thompson, T.E., and T.W. Tillack. 1985. Organization of glycosphingolipids in bilayers and plasma membranes of mammalian cells. *Annu. Rev. Biophys. Chem.* 14:361–386.
- van Meer, G., and K. Simons. 1988. Lipid polarity and sorting in epithelial cells. *J. Cell Biochem.* 36:51–58.
- van Meer, G., E.H. Stelzer, R.W. Wijnaendts van Resandt, and K. Simons. 1987. *J. Cell Biol.* 105:1623–1635.
- van't Hof, W., and G. van Meer. 1990. Generation of lipid polarity in intestinal epithelial (Caco2) cells: sphingolipid synthesis in the Golgi complex and sorting before vesicular traffic to the plasma membrane. *J. Cell Biol.* 111:977–986.
- Venable, J.H., and R. Coggeshal. 1965. A simplified lead citrate stain for use in electron microscopy. *J. Cell Biol.* 25:407–408.
- Vidurgiriene, J., and A.K. Menon. 1994. The GPI anchor of cell-surface proteins is synthesized on the cytoplasmic face of the endoplasmic reticulum. *J. Cell Biol.* 127:333–341.
- Vidurgiriene, J., and A.K. Menon. 1995. Soluble constituents of the ER lumen are required for GPI anchoring of a model protein. *EMBO (Eur. Mol. Biol. Organ.) J.* 14:4686–4694.
- Wandinger-Ness, A., M.K. Bennett, C. Antony, and K. Simons. 1990. Distinct transport vesicles mediate the delivery of plasma membrane proteins to the apical and basolateral domains of MDCK cells. *J. Cell Biol.* 111:987–1000.
- Wilson, J.M., N. Fasel, and J.-P. Kraehenbuhl. 1990. Polarity of endogenous glycosylphosphatidylinositol-anchored membrane proteins in Madin Darby Canine Kidney cells. *J. Cell Sci.* 96:143–149.
- Yoshimori, T., P. Keller, M.G. Roth, and K. Simons. 1996. Different biosynthetic transport routes to the plasma membrane in BHK and CHO cells. *J. Cell Biol.* 133:247–256.
- Zurzolo, C., A. Le Bivic, A. Quaroni, L. Nitsch, and E. Rodriguez-Boulau. 1992. Modulation of transcytotic and direct targeting pathways in a polarized thyroid cell line. *EMBO (Eur. Mol. Biol. Organ.) J.* 11:2337–2344.
- Zurzolo, C., and E. Rodriguez-Boulau. 1993. Delivery of Na⁺, K⁺-ATPase in polarized epithelial cells. *Science*. 260:550–552.
- Zurzolo, C., M.P. Lisanti, I.W. Caras, L. Nitsch, and E. Rodriguez-Boulau. 1993. Glycosylphosphatidylinositol-anchored proteins are preferentially targeted to the basolateral surface in Fischer Rat Thyroid epithelial cells. *J. Cell Biol.* 121:1031–1039.
- Zurzolo, C., W. van't Hof, G. van Meer, and E. Rodriguez-Boulau. 1994. VIP 21/caveolin, glycosphingolipid clusters and the sorting of glycosylphosphatidylinositol-anchored proteins in epithelial cells. *EMBO (Eur. Mol. Biol. Organ.) J.* 13:42–53.